Florence, Italy 12-16 July 2015
ICSV22
The 22nd International Congress on Sound and Vibration

CAA NOISE REDUCTION PARAMETRIC STUDY OF MESH SCREENS APPLIED TO LANDING GEARS

Patrick.N.Okolo, Kun Zhao, Eleonora Neri, John Kennedy and Gareth.J.Bennett

University of Dublin, Trinity College, Ireland.
e-mail: okolop@tcd.ie

Over the years, the environmental and health effects caused by aircraft noise has increased the level of research in this area, with an attempt to address the effects and possibly reduce noise levels associated with the aerodynamic complexities of an aircraft. The major noise source of an aircraft during landing and take-off is generated by large scale aerodynamic turbulent interaction of airstream with the landing gears, both nose and main gears, but majorly at the main landing gear section. This research is a computational aeroacoustics (CAA) study of the noise reduction capabilities of mesh screens applied to landing gears. Unsteady flow past a 2D geometry is simulated with large eddy simulation (LES), using the Smagorinsky subgrid scale model, and the turbulent-induced noise generated at its surface is propagated to far-field receivers with the Ffowcs Williams-Hawkings (FWH) acoustic analogy. The results compared well with documented experimental results. Mesh Screens of 0.46, 0.56 and 0.6 porosities were inserted upstream of the 2D geometry, and noise propagation using Ffowcs Williams-Hawkings (FWH) acoustic analogy showed a reduction in the overall sound pressure levels (OASPL) when these mesh screens are applied. The effect of these mesh screens are studied. A simplified H strut assembly is simulated for turbulent-noise generation prediction, using a Delayed-Detached Eddy Simulation coupled with the FWH acoustic analogy, and the results presented. Overall, we observe the huge potentials of noise prediction using the CFD-FWH Coupled approach, and the turbulent-induced noise reduction capabilities of mesh-screens applied to landing gear arrangements.

1. Introduction

Research aimed at successfully addressing the noise effect of aircrafts started by tackling the most dominant noise source component of aircrafts, which is the engine noise. Therefore, over the years, jet engine noise has reduced significantly. A 15-20 dB jet engine noise reduction between 1970 and 1997 has reduced the average perceived noise level for large commercial aircraft from approximately 110 to 90 EPNdB [1]. However, during approach and landing conditions, throttled back engines, deployed high-lift devices and landing gears often make airframe noise the major contributor to the overall aircraft noise [2]. Aircraft airframe, which comprises of the fuselage, landing gears (main and nose), wings, flaps, slats, etc., has the landing gear noise as its dominant component of noise source during approach and landing conditions, especially for large aircraft [3]. Landing gear arrangement comprises of components with unfavourable aerodynamic features, and the interaction of airflow with

the various protrusions and cavities gives rise to the unsteady flow phenomenon that constitutes a very potent tonal and broadband sound generating mechanism. Therefore, recently, research into various low noise technology schemes applied towards reducing these noise effects without re-designing the aircraft with acoustics as an additional parameter has been ongoing amongst acoustic engineers, researchers and scientists.

The method of shielding landing gear components with fairings and thereby preventing the full interaction of airflow with the various protrusions and cavities had been considered by different research [2, 3]. It was however observed that high speed flow deflection onto other components and the fairing self-noise were the major disadvantages of these fairings. Therefore, bleeding air through these fairings by perforating them can result in a better redistribution of the airflow, and flight tests using these perforated fairings have been conducted [4, 5]. Figure 1 below shows a landing gear model and perforated fairing used for better noise reduction effects compared to a solid non-perforated fairing [6]. Better noise reduction compared to using unperforated fairings were achieved, as shown in Figure 2.

(a) Landing gear model (b) Landing gear model perforated fairings

Figure 1: Landing Gear Model and Perforated Fairing [6]

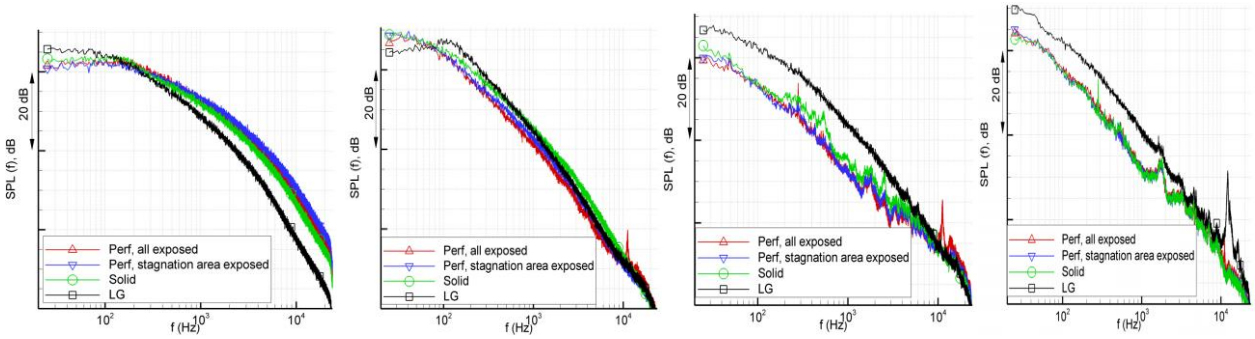

(a) Main Leg Upper (b) Main Leg Lower (c) Bogie-artlink junction (d) Rear bogie cap

Figure 2. Narrowband spectra of on-surface microphones on gear [6]

Recently, instead of using perforated fairings, Oerlemans, et al [7], tested wire mesh screens for noise reduction characteristics on H-Strut beams. Figure 3 below shows an example of the wire mesh screen.

(a) Mesh Screen (b) Mesh cylinder + H-strut

Figure 3. Mesh and H-strut [7]

The principle of flow past a perforated fairing, and wire mesh screen can be seen from the aerodynamics, pressure drop, velocity distribution, turbulence and acoustics point of view. These are summarized as below;

1.1 Pressure drop

Pressure loss coefficient correlation for flow past a perforate is given by Baines [8] as;

(1) $$\zeta = \frac{2\nabla p}{\rho U_\infty{}^2} = \left(\frac{1}{C_c\sigma} - 1\right)^2$$

$values\ of\ C_c\ between\ \frac{2}{3}\ and\ 1$. ζ = pressure loss coefficient, C_c = contraction coefficient, σ = open area ratio. Idelchik [9] further showed that in the turbulent regime of $Re_{d_{or}} \geq 1 \times 10^4$, equation 1 above of is valid for application when using perforated screens. However, for metal wire mesh screens, he showed that;

(2) $$\zeta_{wir} = \frac{2\nabla p}{\rho U_\infty{}^2} = k_0\left(1 - \frac{F_0}{F_1}\right) + \left(\frac{F_0}{F_1} - 1\right)^2 \quad for\ Re = \frac{u_o d_o}{\nu} \geq 10^3$$

Where u_o= velocity in a mesh open section, d_o = diameter of mesh open section, F_0= Area of Clear section, F_1= Area of Mesh. Barlow [10] showed that as a function of mesh screen porosity defined by

(3) $$\beta = \frac{(s-d)^2}{s^2}$$

Where s=open space, and d=thickness of a section, a flow resistance empirical relation is given as;

(4) $$K = K_{mesh}\,K_{Re}(1-\beta) + \left\{\frac{1-\beta}{\beta}\right\}^2$$

This was compared by Oerlemans et al.,[7], and their experimental results of flow resistance roughly agreed with this empirical relation for values of $\beta > 0.4$. $K_{mesh} = 1$, $K_{Re} = 1$ for $Re_d > 400$

1.2 Velocity Distribution

Modification of velocity distribution by perforated plates is treated by Baines [8]. Non uniformities in flow distribution are evened out more by passage through a perforated plate. A theory is developed to predict this modification, which agrees well with experiments for high open area ratios σ > 0.5. Screens with lower values of σ were found to yield unstable flow downstream

1.3 Turbulence

The flow through a screen can be represented by a number of jets that form independently and then gradually spread and coalesce with neighbouring jets. The energy of the mean flow is converted into turbulent energy by eddies produced in the zone of intense shear surrounding each jet. The eddies begin to decay immediately, changing their energy into heat by viscous dissipation. Further downstream the jets are fully mixed and turbulence will become isotropic. The length necessary for decay depends on the jet geometry and therefore scales with d_{or}.

1.4 Acoustics

Perforated plates are often used in acoustic liners as a facing sheet [11]. The facing sheet covers cavities designed to attenuate noise of a particular frequency. Noise that is radiated onto the perforated surface is attenuated due to viscous dissipation in the cavity defined by the perforated surface. Tailoring of the apertures with respect to the expected sound frequency can make for an effective absorption of narrow-band noise. Such perforated surfaces are commonly found in automobile exhaust systems, aircraft engines and compressors.

2. Computational Aero-Acoustics (CAA)

Computational Aero-Acoustics (CAA) can be grouped into two main broad approach. The first approach, is the direct CAA approach, which consists of solving the full compressible equations for the unsteady flow and the acoustic fields simultaneously. This approach is hardly used to analyse cases of engineering interest because of its very high computing power requirements and the need for non-dispersive and non-dissipative schemes to propagate the acoustic waves. If effectively used however, it can account for effects of flow on sound, acoustic reflection, scattering, and can propagate sound through shells, giving a solution of high accuracy. The second based approach, are the hybrid methods, which decouple the fluid dynamics processes acting as noise source generation, from the transport and propagation of the acoustics to a far field domain, making the assumption that the noise generated does not influence the dynamics of the flow. Several methods exist both for the sound generation and for the sound propagation to the far field. For the sound flow generation process, the time-dependency must be accounted for given that aeroacoustics phenomena are intrinsically unsteady. Once the noise sources are known, the sound propagation can be computed via transport equations or acoustic analogies, e.g FWH. Detached Eddy Simulations (DES), and Large Eddy Simulations (LES) are capable of computing the generation of sound and its propagation within the near-field of a landing gear. To propagate the sound to far-field receivers, Ffowcs Williams-Hawkings (FWH) acoustic analogy is used [12]. Progress in Computational Aero-Acoustics (CAA) has led to a number of successful numerical studies of noise generated by complex bodies [13]. The first reported Detached-Eddy Simulation (DES) of the flow over a landing gear was by Hedges et al., [14] in 2002, at a modest Reynolds number Re = 6×10^5. They compared DES with Unsteady Reynolds-Averaged Navier-Stokes (URANS) simulations on a mesh of 2.5×10^6 cells. A highly simplied 31%-scale of a Boeing 757 four-wheel main landing gear was considered. The results were compared with the wind-tunnel experiment of Lazos et al., [15], carried out in the Basic Aerodynamics Research Tunnel (BART) at the NASA Langley Research Centre. Since then, various approaches have been reported to study landing gear noise numerically, with the dominant strategy being a combination of DES and the Ffowcs Williams-Hawkings analogy. Souliez et al,.[16], performed simulations on a four-wheel LG bogie model, coupled with the FWH integral equation for far-field propagation.

2.1 Theory of Acoustic Analogy

Lighthill [17] introduced the wave equation of acoustic analogy having the source derived by comparing the exact equations of motion of a fluid with the equations of sound propagation in a medium at rest as follows

$$\frac{1}{c^2}\frac{\partial^2 \rho'}{\partial t^2} - \nabla^2 \rho' = \frac{\partial^2 T_{ij}}{\partial x_i \partial x_j} \tag{5}$$

$$T_{ij} = \rho v_i v_j + p_{ij} - c^2 p' \delta_{ij} \tag{6}$$

Where ρ' = density perturbation, T_{ij} = lighthill's stress tensor, p_{ij} = compressive stress tensor, c= velocity of sound in fluid at rest, v_i= velocity component in x_i direction.

Curle [18], extended lighthill's analogy considering a rigid surface, while Ffowcs Williams and Hawkings further expanded it to include the effects of a rigid body in arbitrary motion.

Farassat [19], developed the FW-H analogy equation into integral forms for the monopole, dipole and quadrupole source terms.

3. Configuration and Computational Grid

3.1 2D Cylinder

In the present work, the noise produced by the fluid when it passes over the cylinder is found by means of CAA models. So our interest turns towards the prediction of acoustic fields on flow past a

circular cylinder using CAA model. In this model, the acoustic source data is extracted from a transient LES based on Smagorinsky subgrid scale model. Receiver locations of reciever1-(0,-35D) and reciever2-(0,-128D) are used for the noise measurement locations. The 2D cylinder size, computational domain, and mesh are as shown below. Cylinder diameter D=0.019m, $Re_D = 9 \times 10^4$, computational domain extends 5D upstream and 20D downstream of cylinder, with height of 20D. Mesh size= 483958 cells.

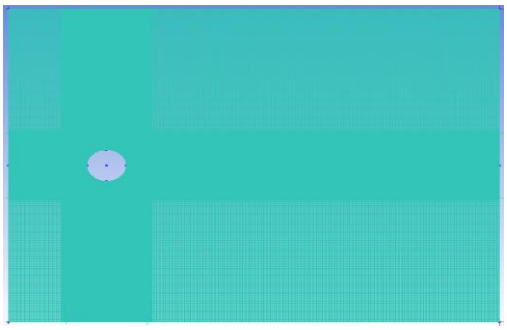

Figure 4 (a) Cylinder Mesh Domain

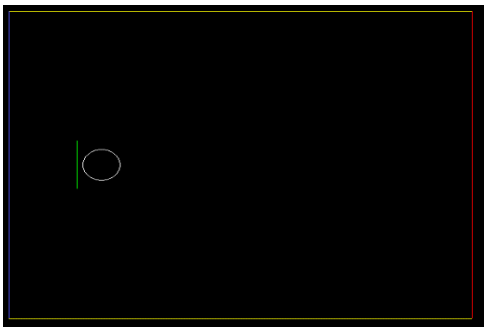

Figure 4 (b) Mesh Domain Showing Porous Cell

3.2 3D H-Strut

The lack of substantial documented CFD results for unsteady flows past H-shaped beams and struts limits the comparison of this CAA simulation to only the experiment performed by Oerlemans[7]. For the flow simulation past the 3D strut, the Delayed-Detached Eddy Simulation (DDES) is used, where the Spalart-Allmaras RANS model is used for the near wall region. The computational domain is min(-0.295, -0.165, 0) and max(1.505, 0.215,0.7). mesh size= 514,095 cells.

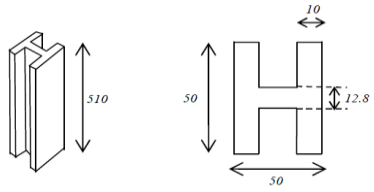

Figure 5 (a) Strut dimension

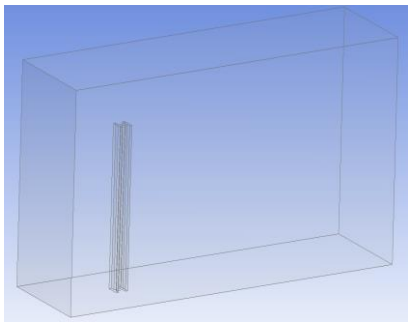

(b) Computational Domain

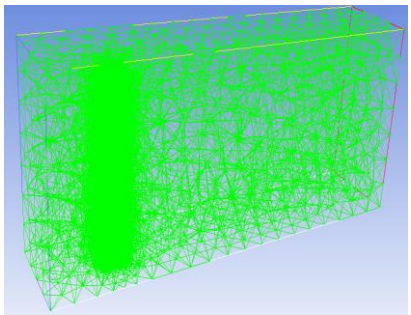

(c) Computational Mesh

To simulate the effect of the introduction of a mesh screen upstream of our bluff body, we define a porous cell zone in our computational domain, and define the pressure resistance drop across the cell zone, and its porosity. The Porous cell media is modelled by the addition of a momentum source term to the standard fluid flow equations. The source term is composed of two parts, a viscous loss term, and an inertial loss term.

$$S_i = -\left(\sum_{j=1}^{3} D_{ij}\mu v_j + \sum_{J=1}^{3} C_{ij}\frac{1}{2}\rho|v|v_j\right) \tag{7}$$

Where S_i is the source term for the i-th (x, y,or z) momentum equation, $|v|$ is the magnitude of the velocity and D and C are prescribed matrices, which are user-defined empirical coefficients. For the porous mesh screen used in this research, the empirical relation of pressure normalized flow resistance by barlow[10], Eqs. (4) is used to get our user-defined empirical coefficients.

4. Results

Results for the 2D cylinder flow, for the no mesh screen case, 0.6, 0.56 and 0.46 porosity cases are presented. Receiver locations of reciever1-(0,-35D) and reciever2-(0,-128D) are used for the noise measurement locations.

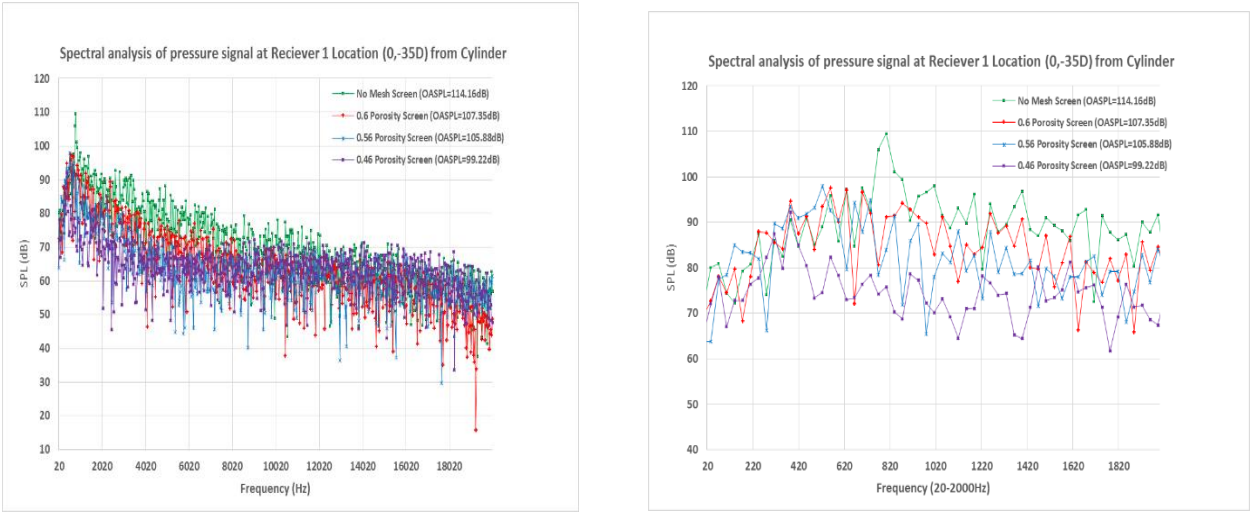

Figure 6 Receiver 1 Spectral Analysis

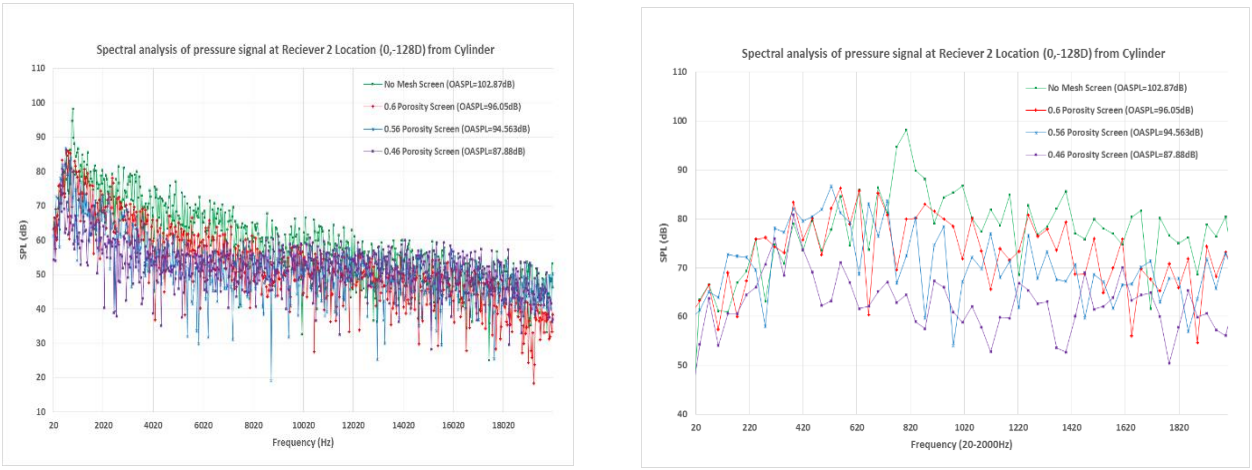

Figure 7 Receiver 2 Spectral Analysis

The results of the 2D cylinder flow simulations were compared with the experimental results of Revel et al,.[20], in which was recorded 117dB, and 100dB OASPL at receiver 1 and receiver 2 locations respectively. The spectrum peaks at a strouhal number of 0.21, which also compares well with experimental data of 0.19. From the plots shown, we notice that the mesh screens cause a reduced turbulent-induced noise from the 2D cylinder.

Velocity and vorticity magnitude at locations x=0.001 and y ranging from -0.05 and 0.05, upstream and downstream of the cylinder were probed, and the results presented in Figure. 8 below.

From these probe locations, we observe that the porous mesh screens effectively reduced the local fluid flow speeds impacting the cylinder, which leads to noise reduction. Since the turbulent-induced aerodynamic noise from bluff bodies generally scales with the 6^{th} power of flow speed, this becomes one of the mechanisms which is responsible for the reduced noise. Also, we observe that the vorticity increases upstream of the cylinder due to the introduction of the mesh screens, with the mesh screen of 0.46 porosity introducing the highest amount of vorticity upstream the cylinder, and also causing a higher reduced amount of turbulent-induced noise.

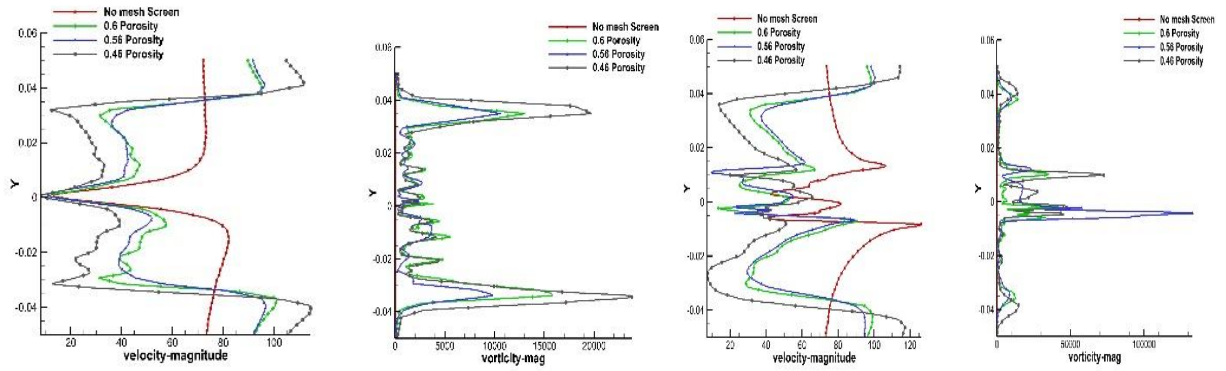

Figure 8 (a) Upstream of 2D Cylinder **(b)** Downstream of 2D Cylinder

Therefore, we see that the mesh screens break up the incoming flow into small amount of vortices, increasing the vorticity upstream of the cylinder, and hence further affecting turbulent-induced noise generation mechanism. More research is needed to better understand this effects.

Results for the turbulent-induced noise from the H-strut is presented, and compared with the experimental results of Orelemans, et al,.[7]. Receiver locations of reciever1-(0,-0.7,0), reciever2-(0,-0.7, 0.51) and (0, 0.7, 0.7) are used for the noise measurement locations.

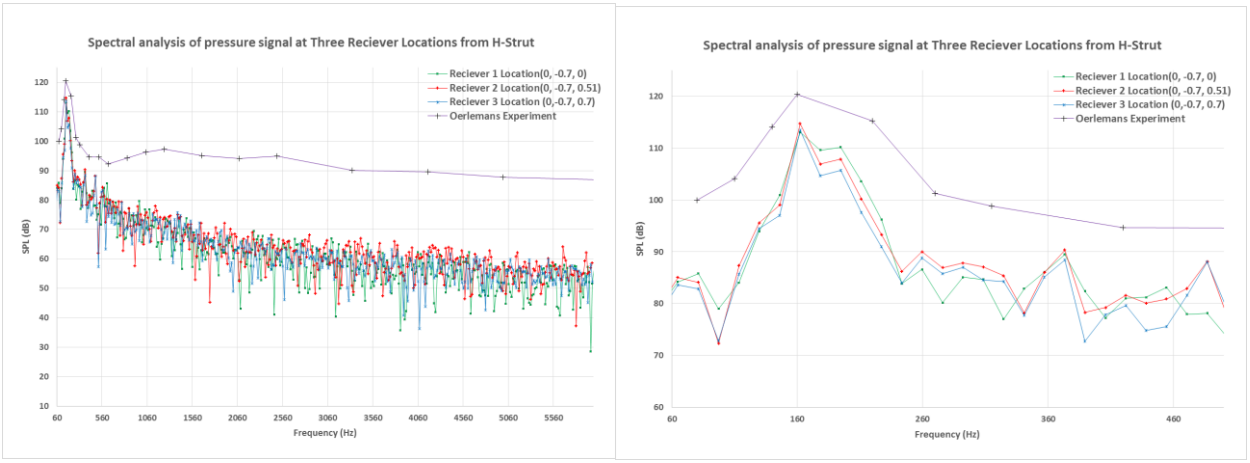

Figure 9. Comparison of SPL Results for 3D strut (70m/s $\alpha = 0°$)

Comparing our results with the experimental data, our CAA approach predicted the vortex shedding peak at 162.34Hz, and a corresponding Strouhal number of 0.114. Which is close to the experimental data of 160Hz peak frequency and a Strouhal number of 0.11. However, this prediction approach compared reasonably well only with low frequency noise. This could possibly be due to the fact that the numerical near-wall grid was not fine enough to accommodate all turbulent scales.

5. Conclusion

Computational aeroacoustics study of the noise reduction capabilities of mesh screens applied to landing gears have been investigated. LES using the Smagorinsky subgrid scale model for flow past a 2D cylinder, was coupled with the acoustic analogy of Ffowcs Williams-Hawkings (FWH), and the turbulent-induced noise sources at its surface propagated to far-field receivers. Mesh Screens of 0.46, 0.56 and 0.6 porosities were inserted upstream of the 2D geometry to study their noise reduction characteristics. We observed a reduction in the overall sound pressure levels (OASPL) when these

mesh screens are applied. The effect of these mesh screens were seen in the local flow, as they effectively reduced the local fluid flow speeds impacting the cylinder, leading to noise reduction, because the turbulent-induced aerodynamic noise from bluff bodies generally scales with the 6th power of flow speed. Also, these mesh screens introduce vortices into the flow which affects the noise generation mechanism in the vortex shedding region of the cylinder. More research will be done to fully understand the true nature of this noise reduction effects of mesh screens. Delayed-Detached Eddy Simulation was also carried out on a simplified 3 dimensional H-strut assembly, and coupled with the FWH Acoustic analogy for turbulent-noise generation prediction. Overall, we observe the huge potentials of noise prediction using CAA, and the turbulent-induced noise reduction capabilities of mesh-screens applied to landing gears.

REFERENCES

[1] Ross, J.C. Progress in airframe noise reduction. In Canadian Aeronautics and Space Institute Annual Conference, 2001.

[2] Dobrzynski , W, Chow , L.C., Guion P., and Shiells, D. A European study on landing gear airframe noise sources. AIAA Paper 2000–1971, 2000

[3] Dobrzynski, W. and Buchholz, H.. Full-scale noise testing on Airbus landing gears in the German Dutch wind tunnel. AIAA Paper 97–1597, 1997

[4] Piet, J.-F., Chow , L.C, Laporte , F and Remy , H.. Flight test investigation of high-lift devices and landing gear modifications to achieve airframe noise reduction. In ECCOMAS 2004 conference, Jyvaeskylae, Finland, July 2004.

[5] Piet, J.-F, Davy, R. Elias, G., Siller, H.A. Chow , L.C, . Seror , C, and Laporte , F. Flight test investigation of add-on treatments to reduce aircraft airframe noise. AIAA Paper 2005–3007, 2005.

[6] Boorsma, K. (2008). "Aeroacoustic Control of Landing Gear Noise using Perforated Fairings". University Of Southampton, School Of Engineering Sciences Aerodynamics and Flight Mechanics Research Group, PhD Thesis, pages 1-33.

[7] Oerlemans, S., Sandu, C., Molin , N. and Piet , J.F., "Reduction of Landing Gear Noise using Mehes" AIAA paper 2010-3972, 2010.

[8] Baines , W.D. and Peterson , E.G.. An investigation of flow through screens. Transactions of the ASME, Journal of Applied Mechanics, 73:467–478, 1951.

[9] Idelchik, I.E.. Handbook of Hydraulic Resistance. Third Edition, 1994.

[10] Barlow, J. B., Rae, W. H., and Pope, A., "Low-speed wind tunnel testing," third edition, Wiley, 1999.

[11] Chen, W., Lee , F., and Chiang, D.. On the acoustic absorption of porous materials with different surface shapes and perforated plates. Journal of Sound and Vibration, 237(2):337–355, 2000.

[12] Ffowcs Williams ,J. E,. and Hawkings, D. L., , "Sound Generation by Turbulence and Surface in Arbitrary Motion," Philosophical Transactions of the Royal Society of London. Series A, Mathematical and Physical Sciences, Vol. 264, No. 1151, 1969, pp. 321-342.

[13] Wang, M., Freund , J. B.,, and Lele , S. K, "Computational Prediction of Flow-Generated Sound," Annu. Rev. Fluid Mech., Vol. 38, 2006, pp. 483-512.

[14] Hedges , L. S., Travin , A. K., and Spalart, P. R. "Detached-Eddy Simulations Over a Simplified Landing Gear," J. Fluids Eng., Vol. 124, 2002, pp. 413-423.

[15] Lazos , B. S., "Mean Flow Features Around the Inline Wheels of Four-Wheel Landing Gear," AIAA J., Vol. 40, No. 2, 2002, pp. 193-198.

[16] Souliez, F. J., Long, L. N., Morris, P. J, and Sharma A., "Landing Gear Aerodynamic Noise Prediction Using Unstructured Grids," 40th AIAA Aerospace Sciences Meeting & Exhibit, 2002.

[17] Lighthill, M. J., "On Sound Generated Aerodynamically. I. General Theory," Philosophical Transactions of the Royal Society of London. Series A, Mathematical and Physical Sciences, Vol. 211, 1952, pp. 564-587.

[18] Curle , N., "The Influence of Solid Boundaries upon Aerodynamic Sound Philosophical Transactions of the Royal Society of London. Series A, Mathematical and Physical Sciences, Vol. 231, 1955, pp. 505-514.

[19] Farassat, F. and Brentner, K.S. (1988) Supersonic Quadrupole Noise Theory for High-speed Helicopter Rotors. *Journal of Sound and Vibration*, **218**, 481-500.

[20] Revell, J.D., Prydz, R.A., and Hays, A.P., "Experimental Study of Airframe Noise vs. Drag Relationship for Circular Cylinders," *Lockheed Report 28074, Feb. 1977. Final Report for NASA Contract NAS1-14403*.